nature geoscience

LETTERS

PUBLISHED ONLINE: 13 APRIL 2014 | DOI: 10.1038/NGEO2137

Low palaeopressure of the martian atmosphere estimated from the size distribution of ancient craters

Edwin S. Kite[1*†], Jean-Pierre Williams[2], Antoine Lucas[1] and Oded Aharonson[1,3]

The decay of the martian atmosphere—which is dominated by carbon dioxide—is a component of the long-term environmental change on Mars[1] from a climate that once allowed rivers to flow[2–6] to the cold and dry conditions of today. The minimum size of craters serves as a proxy for palaeopressure of planetary atmospheres, because thinner atmospheres permit smaller objects to reach the surface at high velocities and form craters[7–9]. The Aeolis Dorsa region near Gale crater on Mars contains a high density of preserved ancient craters interbedded with river deposits[11] and thus can provide constraints on atmospheric density at the time of fluvial activity. Here we use high-resolution images and digital terrain models[10] from the Mars Reconnaissance Orbiter to identify ancient craters in deposits in Aeolis Dorsa that date to about 3.6 Gyr ago and compare their size distribution with models of atmospheric filtering of impactors[12,13]. We obtain an upper limit of 0.9 ± 0.1 bar for the martian atmospheric palaeopressure, rising to 1.9 ± 0.2 bar if rimmed circular mesas—interpreted to be erosionally-resistant fills or floors of impact craters—are excluded. We assume target properties appropriate for desert alluvium[14]: if sediment had rock-mass strength similar to bedrock at the time of impact, the paleopressure upper limit increases by a factor of up to two. If Mars did not have a stable multibar atmosphere at the time that the rivers were flowing—as suggested by our results—then a warm and wet CO_2/H_2O greenhouse[2] is ruled out, and long-term average temperatures were most likely below freezing.

Planetary atmospheres brake, ablate and fragment small asteroids and comets, filtering out small high-velocity surface impacts and causing fireballs, airblasts, meteors and meteorites. The smallest impact craters near sea level on Earth have diameter $D \sim 20$ m. 'Zap pits' as small as 30 μm are known from the airless Moon, but other worlds show the effects of progressively thicker atmospheres: the modern martian atmosphere can remove >90% of the kinetic energy of >240 kg impactors[7]; Titan's paucity of small craters is consistent with atmospheric filtering of craters smaller than 6–8 km (ref. 8); and on Venus, craters $D < 20$ km are substantially depleted by atmospheric effects[9].

Changes in the concentration of atmospheric volatiles are believed to be the single most important control on the climate evolution and habitability of Mars, which in turn is a benchmark for habitable-zone calculations for exoplanets[15]. Contrary to early work[2], it is doubtful that increasing CO_2 pressure (≈total atmospheric pressure, P) is enough to raise the mean annual surface temperature ($\overline{T}$) of early Mars to the freezing point, even when water vapour and cloud feedbacks are considered[5]. However, increased CO_2 aids transient surface liquid water production by impacts, volcanism, or infrequent orbital conditions[3,4,6]. Existing data require an early epoch of massive atmospheric loss to space, suggest that the present-day rate of escape to space is small, and offer evidence for only limited carbonate formation[16]. These data have not led to convergence among atmosphere evolution models, which must balance poorly understood fluxes from volcanic degassing, escape to space, weathering and photolysis[17]. More direct measurements[18] are required to determine the history of Mars's atmosphere. Wind erosion exposes ancient cratered volumes on Mars and the size of exhumed craters has been previously suggested as a proxy of ancient Mars P (for example, ref. 19).

Here we obtain a new upper limit on the atmospheric pressure of early Mars from the size–frequency distribution of small ancient craters (Fig. 1) interspersed with river deposits in Aeolis, validated using High Resolution Imaging Science Experiment (HiRISE) digital terrain models (DTMs) and anaglyphs, in combination with simulations of the effect of P on the crater flux. The craters are interbedded with river deposits up to $\sim 10^3$ km long, with inferred peak river discharge 10–1,000 m^3 s^{-1} (ref. 10). Therefore, the atmospheric state they record corresponds to an interval of time when Mars was substantially wetter than the present, probably >3.6 Gyr ago (Ga) (Supplementary Methods).

Aeolis Dorsa (part of the Medusae Fossae Formation) is a promising location to hunt for ancient craters: the stratigraphy contains numerous channel-fill deposits of large rivers and, when these overlie a crater, that crater must be as ancient as the rivers[20]. Certain beds in Aeolis Dorsa (Supplementary Methods) preserve a high density of ancient craters, perhaps due to slow deposition or a diagenetic history unusually favourable for crater preservation. We constructed stereo DTMs/orthophotos for two image pairs covering these beds, DTM1 and DTM2 (Methods). Following a checklist (Supplementary Table), craters were classified as definite ancient craters (visibly embedded within stratigraphy: for example, overlain by river deposit; $n = 56$, median diameter $D_{50} = 107$ m, 10th-percentile diameter $D_{10} = 50$ m), rimmed circular mesas (RCMs; $n = 71$, $D_{50} = 48$ m, $D_{10} = 21$ m), or candidate ancient crater ($n = 192$, D_{50} also 48 m, D_{10} also 21 m; candidates are not considered further, but their inclusion would strengthen our conclusions). We measured D by fitting circles to preserved edges/rims. RCMs appear as disks in raw HiRISE images. We interpret them as the erosionally resistant fills/floors of impact craters that were topographically inverted during the deflation of the target unit. They are unlikely to be

[1]Geological and Planetary Sciences, Caltech, California 91125, USA, [2]Earth and Space Sciences, University of California, Los Angeles, California 90025, USA, [3]Helen Kimmel Center for Planetary Science, Weizmann Institute of Science, Rehovot 76100, Israel. †Present address: Princeton University, Princeton, New Jersey 08544, USA. *e-mail: ekite@princeton.edu

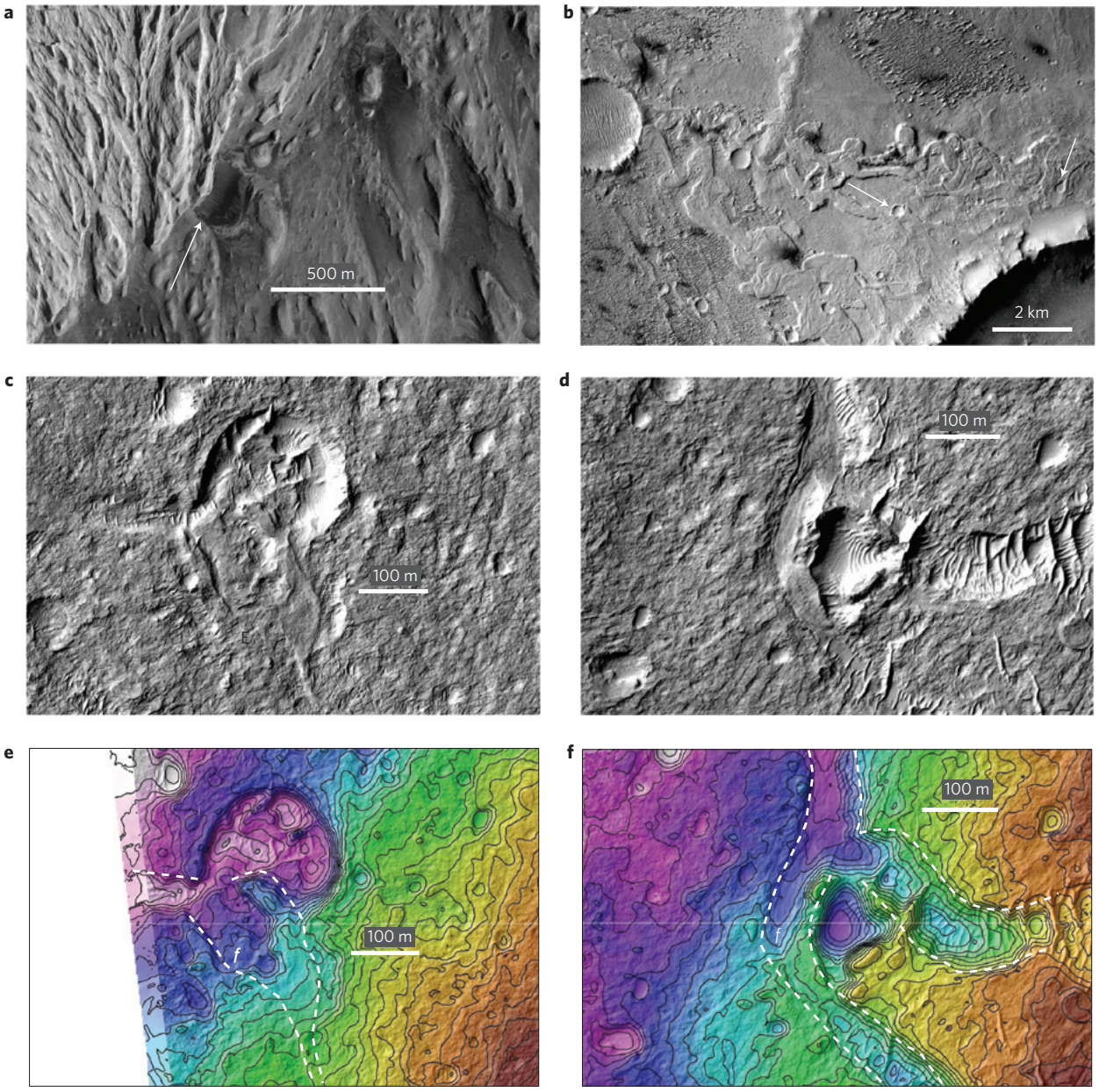

Figure 1 | Gallery of ancient martian craters (from ref. 20). a, Crater being exhumed from beneath an unconformity within Gale crater's mound (Aeolis Mons/Mount Sharp), the destination of the Curiosity rover. ESP_019988_1750. **b**, Craters with intact rims being exhumed from beneath meander belts, Aeolis Dorsa, G03_019249_1744_XI_05S205W; ref. 10. **c**, Crater partly draped by fluvial channel materials (*f* in **e**), Aeolis Dorsa. Diameter, 238 m. ESP_019104_1740. **d**, Crater partly draped by fluvial channel materials (*f* in **f**), Aeolis Dorsa, ESP_019104_1740. Diameter, 141 m. **e**, Crater from **c**, but with 1 m elevation contours from DTM2 (see text). **f**, Crater from **d** with 1 m contours from DTM2.

outliers of a young mantle because they are not found away from the fluvial unit. We plot them separately, but consider them to be probable ancient craters. We used unambiguously ancient craters as a guide to the preservation state of the smaller craters. These ancient craters are unlikely to be maars; maars are not randomly distributed in space or time/stratigraphy. We also reject the possibility that they are palaeokarst sinkholes; sinkholes lack rims, are concentrated at particular stratigraphic levels, and are overdispersed.

We generated synthetic crater populations for varying P (ref. 12). The approach is conceptually similar to that of previous studies[13] and benefits from measurements of the present martian cratering flux (Methods). Modelled smallest-crater diameter increases linearly with pressure (~20 m at 1 bar) as expected from equating impactor and atmospheric-column masses[21]. This is broadly consistent with low-elevation impacts on Earth (the column mass of Earth's sea-level atmosphere is equivalent to ~0.4 bar on Mars). We apply a geometric correction for exhumation from a cratered volume (Supplementary Methods) assuming that initial crater shape is isometric over the diameter range. After bayesian fitting, we correct our P estimate for elevation (our DTMs are below datum; Mars's average P was 20% lower than local P).

We compared the model with the combined data set (DTM1 + DTM2). Combined best fits are $P = 1.9 \pm 0.2$ bar, falling to $P = 0.9 \pm 0.1$ bar if RCMs are also included (Fig. 2). As better preservation/exposure could allow still smaller embedded craters to be uncovered, we interpret our fits as upper limits. The best fit to DTM1 (DTM2) ancient craters alone is 1.7 ± 0.3 bar (2.2 ± 0.3 bar), falling to 0.8 ± 0.1 bar (0.9 ± 0.1 mbar) if RCMs are included.

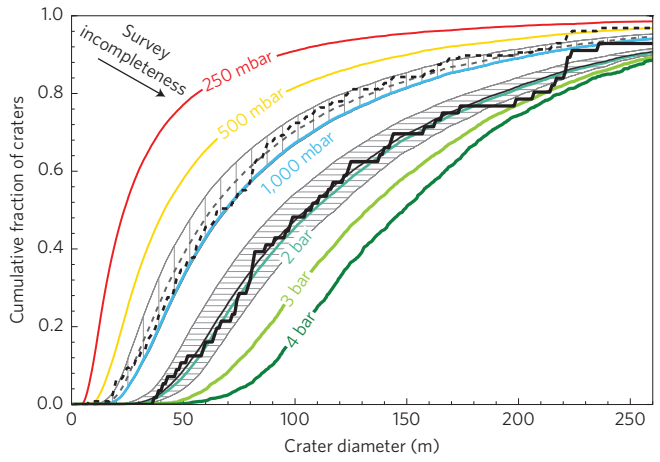

Figure 2 | Upper limits on the atmospheric pressure of early Mars. Comparison of model crater size–frequency distributions to observations. Solid black line corresponds to definite embedded craters. Dashed black line additionally includes rimmed circular mesas. Stair-stepping in the data curves corresponds to individual craters. Coloured lines show model predictions for atmospheric filtering of small impactors at different pressures. Grey hatched regions correspond to 2σ statistical error envelopes around the best-fit palaeopressure to the data (best fits shown by thick grey lines). Survey incompleteness leads to overestimates of median crater size, so best fits are upper limits.

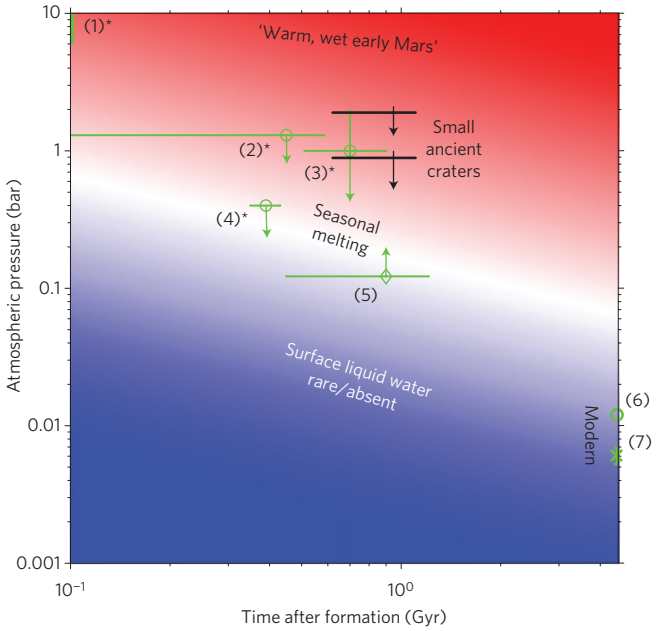

Figure 3 | Palaeopressure constraints on the great drying of Mars. Black symbols are the result from this work. Green symbols are other estimates (asterisks mark indirect estimates): (1*) cosmochemical estimate[26]; (2*) prehnite stability; (3*) carbonate Mg/Ca/Fe (ref. 27); (4*) $^{40}Ar/^{36}Ar$ (ref. 32); (5) bomb sag[18]; (6) modern atmosphere; (7) modern atmosphere + CO_2 ice. Approximate and model-dependent implications for sustained surface habitability are shown by background colours (blue, always below freezing; red, year-round melting; slope schematically shows the effect of the fainter young sun). 'Warm, wet early Mars' refers to the stable climate solution in ref. 2. Age estimates are detailed in Supplementary Methods.

The results are sensitive to target strength, as expected[22]. Increasing the target rock-mass strength to a hard-rock-like 6.9 MPa (ref. 23) while holding all other parameters constant increases the combined (including RCMs) upper limit on P to ∼2 bar (Supplementary Methods). Figure 2 assumes weak soil-like target strength appropriate for river alluvium in an aggrading sedimentary deposit: if sediment developed bedrock-like rock-mass strength by early diagenesis, the upper limit is greatly increased. Sensitivity tests show a relatively minor effect of fragmentation on the results (Supplementary Methods).

We do not consider crater shrinkage or expansion by crater degradation. Only shrinkage matters for the purpose of setting an upper bound on P: as the crater is abraded, the exposed radius must eventually vanish. We surmise that shrinkage is a small effect because impact craters are bowl-shaped (as opposed to cone-shaped) and because rims are frequently preserved.

Our technique rules out a thick, stable palaeoatmosphere and cannot exclude atmospheric collapse–reinflation cycles on timescales much shorter than the sedimentary basin-filling time. General circulation models predict that atmospheric collapse to form CO_2 ice sheets and subsequent reinflation might be triggered by obliquity change[5]. If sediment accumulated at 1–100 μm yr^{-1} (ref. 20), our DTMs could integrate over $\sim 10^6$–10^8 years of sedimentation and contain many collapse–reinflation cycles. Therefore one interpretation is that smaller ancient craters formed while the atmosphere was collapsed, whereas rivers formed during high-obliquity, thick-atmosphere intervals. However, published models indicate that collapse to form polar CO_2 ice sheets occurs only for pressures less than our upper limit[5]. If these models are correct, then our pressure constraint is a true upper bound on typical atmospheric pressure.

Downward revisions to the infrared opacity of CO_2 indicate that any amount of CO_2 is insufficient to warm early Mars $\overline{T}$ to the freezing point[5]. Even if further work incorporating radiatively active clouds[24] moderates this conclusion, our result is an independent constraint on stable CO_2/H_2O warm–wet solutions (Fig. 3). However, increased CO_2 below the warm–wet threshold primes the climate of Mars for surface liquid water production by other relatively short-lived mechanisms, by adding to the greenhouse effect, pressure-broadening the absorption lines of other gases[4], suppressing evaporitic cooling[6] and increasing atmospheric heat capacity[3].

If the small-crater limit is representative of early Mars P, it is difficult to envisage continuous stability of surface liquid water for the 10^4–10^5 yr needed to allow water to cycle between deep aquifers and the surface. This is true even with optimistic CO_2 radiative forcing parameterizations. Transient warming by eruptions, impacts, or infrequent orbital conditions could unfreeze the surface and shallow subsurface, allowing runoff, but would not last long enough to unfreeze ground at ∼1 km depth. Therefore, CO_2/H_2O atmospheric models do not support $\overline{T}$ above freezing on early Mars, which has implications for sedimentary rock formation and diagenesis, habitability and groundwater hydrology. (A recent study[25] shows that mean temperatures above the freezing point are marginally consistent with our result, but only if the early Mars atmosphere contained ≥20% H_2).

Atmospheric loss must be part of the explanation for Mars's great drying, if only because freshwater rivers cannot flow for hundreds of kilometres when simultaneously boiling and freezing. How high P was, and its decay over time, are not known. The 2014–2015 Mars Atmosphere and Volatile Evolution (MAVEN) mission will measure modern loss processes, which is complementary to our geologic palaeoproxy approach.

Mars would have formed with ≥6–10 bars CO_2 equivalent of carbon assuming the same initial [C] and [Kr] as Earth. $^{40}Ar/^{36}Ar$ and $^{129}Xe/^{132}Xe$ suggest that 90–99% of the initial atmosphere was lost before ∼4.1 Ga (ref. 26). Subsequent loss rates are less clear; Mars's $C/^{84}Kr$ ratio suggests $P \sim 60$ mbar following the Late Heavy Bombardment[26].

Ref. 18 uses a volcanic bomb sag in Gusev crater to infer $P > 120$ mbar from the bomb sag's terminal velocity. This is consistent with our result. Our small-crater constraints on early Mars atmospheric pressure are also congruent with isotopic and mineralogic indicators, which generally require more assumptions than our method. For example, prehnite is observed on Mars and is unstable for CO_2 mixing ratios $> 2 \times 10^{-3}$. This implies $P \lesssim 1$ bar, but only if water at depth was in equilibrium with the atmosphere. The composition of a carbonate-rich outcrop at Gusev has been interpreted to require $P = 0.5$–2 bar assuming that the carbonates are a solid solution in thermodynamic equilibrium[27]. Models[16] of volcanic degassing, escape of CO_2 and impact delivery also hint that the atmospheric pressure on Mars at the time of the Late Heavy Bombardment was not greater than our estimate.

In the future, pyroclastic-blast runout length or even rainsplash[28] could be used to constrain P. Curiosity's field site in Gale crater contains syndepositional craters (Fig. 1a), so Curiosity could validate orbital identifications of embedded craters along its traverse. The 40-year-old prediction of a connection between drying and atmospheric decay could be tested by applying the small-crater technique to sedimentary deposits of different ages—ranging from Mawrth (the oldest known sedimentary sequence in the Solar System), through Meridiani, to the relatively young Valles Marineris silica deposits. This could yield a time series of constraints on the atmospheric pressure of early Mars, stratigraphically coordinated to the sedimentary record of Mars's great drying.

Methods

DTM generation. DTMs were constructed following ref. 11 from HiRISE images PSP_007474_1745/ESP_024497_1745 (DTM 1) and ESP_017548_1740/ESP_019104_1740 (DTM 2). Mars Orbiter Laser Altimeter Precision Experiment Data Records were used as ground control points. Optimal resolution depends on HiRISE image map scale (0.25–0.5 m), giving 1–2.5 m per post DTMs. Vertical precision is ~0.3 m, with 90% probability of precision $\lesssim$1 m (Supplementary Methods).

Cratering model. We built a synthetic impactor population by drawing randomly from distributions of material types, densities and ablation coefficients, which are set based on terrestrial fireball network observations (the model assumes the same fractional distribution at Mars). Details of the cratering model, including the sources for parameter choices, are given in the Supplementary Methods. We advect these populations to the surface through atmospheres with scale height 10.7 km. The code does not track planet curvature; we do not allow impactors to skip back to space. The atmosphere drains kinetic energy from impactors through drag (per unit mass):

$$dv/dt = C_D\ \rho_a v^2 A$$

(we assume a drag coefficient $C_D = 1$ across the velocity (v) and size range of interest) and ablation:

$$dm/dt = (C_h\ \rho_a\ v^3 A)/2\zeta$$

where t is time, m is mass, ρ_a is local atmospheric density, A is cross-sectional area, C_h is the heat transfer coefficient and ζ is the heat of ablation. Particles braked to <500 m s^{-1} would not form hypervelocity craters and are removed from the simulation. We do not track secondary craters, because metre-sized endoatmospheric projectiles are likely to be braked to low speeds for the relatively thick atmospheres we are evaluating. In other words, if wet-era small craters are secondaries, then the atmosphere of early Mars was thin. Transient impact-induced increases in P would not affect our upper limit; transient local decreases in P could conceivably enhance secondary flux. It has been suggested that unrecognized secondary craters significantly contribute to all counts of $D < 1$ km martian craters[29] and, although it has been shown by others that unrecognized secondaries are not required to explain observed crater size–frequency distributions[12,30,31], the small-crater-rich size-frequency distribution of secondaries (if pervasively present with high relative frequency on all martian surfaces, as suggested by ref. 29) could mimic the effect of a lower atmospheric pressure. Crater sizes are calculated using π-group scaling[23], assuming a target strength of 65 kPa and a target density of 2,000 kg m^{-3} appropriate to cohesive desert alluvium[14], with the Holsapple scaling parameters $k_1 = 0.132$, $k_2 = 0.26$, $k_r = 1.1$ and $\mu = 0.41$. We adopt the values in keith.aa.washington.edu/craterdata/scaling/theory.pdf; note that the value $k_1 = 0.24$ given in Table 1 of ref. 23 is in error (K. A. Holsapple, personal communication).

Received 31 August 2013; accepted 10 March 2014; published online 13 April 2014

References

1. Mahaffy, P. R. *et al.* Abundance and isotopic composition of gases in the martian atmosphere from the Curiosity rover. *Science* **341,** 263–266 (2013).
2. Pollack, J. B., Kasting, J. F., Richardson, S. M. & Poliakoff, K. The case for a wet, warm climate on early Mars. *Icarus* **71,** 203–224 (1987).
3. Segura, T. L., Toon, O. B. & Colaprete, A. Modeling the environmental effects of moderate-sized impacts on Mars. *J. Geophys. Res.* **113,** E11007 (2008).
4. Tian, F. *et al.* Photochemical and climate consequences of sulfur outgassing on early Mars. *Earth Planet. Sci. Lett.* **295,** 412–418 (2010).
5. Forget, F. *et al.* 3D modelling of the early martian climate under a denser CO_2 atmosphere: Temperatures and CO_2 ice clouds. *Icarus* **222,** 81–99 (2013).
6. Kite, E. S., Halevy, I., Kahre, M. A., Wolff, M. J. & Manga, M. Seasonal melting and the formation of sedimentary rocks on Mars, with predictions for the Gale crater mound. *Icarus* **223,** 181–210 (2013).
7. Chappelow, J. E. & Golombek, M. P. Event and conditions that produced the iron meteorite Block Island on Mars. *J. Geophys. Res.* **115,** E00F07 (2010).
8. Wood, C. A. *et al.* Impact craters on Titan. *Icarus* **206,** 344–344 (2010).
9. Herrick, R. R., Sharpton, V. L., Malin, M. C., Lyons, S. N. & Feely, K. in *Venus II* (eds Bougher, S. W., Hunten, D. M. & Phillips, R. J.) 1015–1046 (Univ. Arizona Press, 1997) (catalogue as v3; updated by R. R. Herrick in http://www.lpi.usra.edu/resources/vc/vchome.html).
10. Burr, D. M. *et al.* Inverted fluvial features in the Aeolis/Zephyria Plana region, Mars: Formation mechanism and initial paleodischarge estimates. *J. Geophys. Res.* **115,** E07011 (2010).
11. Kirk, R. L. *et al.* Ultrahigh resolution topographic mapping of Mars with MRO HiRISE stereo images: Meter-scale slopes of candidate Phoenix landing sites. *J. Geophys. Res.* **113,** E00A24 (2008).
12. Williams, J-P., Pathare, A. & Aharonson, O. *Modeling Small Impact Populations on Mars, EPSC Abstracts, Vol. 7* (European Planetary Science Congress, 2012).
13. Popova, O., Nemtchinov, I. & Hartmann, W. K. Bolides in the present and past martian atmosphere and effects on cratering processes. *Meteorit. Planet. Sci.* **36,** 905–925 (2003).
14. Holsapple, K. A. & Housen, K. R. A crater and its ejecta: An interpretation of Deep Impact. *Icarus* **191,** 586–597 (2007).
15. Kopparapu, R. K. *et al.* Habitable zones around main-sequence stars: New estimates. *Astrophys. J.* **765,** 131 (2013).
16. Lammer, H. *et al.* Outgassing history and escape of the martian atmosphere and water inventory. *Space Sci. Rev.* **174,** 113–154 (2013).
17. Manning, C. V., McKay, C. P. & Zahnle, K. J. Thick and thin models of the evolution of carbon dioxide on Mars. *Icarus* **180,** 38–59 (2006).
18. Manga, M., Patel, A., Dufek, J. & Kite, E. S. Wet surface and dense atmosphere on early Mars inferred from the bomb sag at Home Plate, Mars. *Geophys. Res. Lett.* **39,** L01202 (2012).
19. Vasavada, A. R., Milavec, T. J. & Paige, D. A. Microcraters on Mars: Evidence for past climate variations. *J. Geophys. Res.* **98,** 3469–3476 (1993).
20. Kite, E. S., Lucas, A. S. & Fassett, C. I. Pacing early Mars river activity: Embedded craters in the Aeolis Dorsa region imply river activity spanned $\gtrsim$(1–20 Myr). *Icarus* **225,** 850–855 (2013).
21. Melosh, H. J. *Impact Cratering: A Geologic Process* (Oxford Monographs on Geology and Geophysics Series, Vol. 11, Clarendon Press, 1989).
22. Dundas, C. M., Keszthelyi, L. P., Bray, V. J. & McEwen, A. S. Role of material properties in the cratering record of young platy-ridged lava on Mars. *Geophys. Res. Lett.* **37,** L12203 (2010).
23. Holsapple, K. A. The scaling of impact processes in planetary sciences. *Ann. Rev. Earth Planet. Sci.* **21,** 333–373 (1993).
24. Urata, R. A. & Toon, O. B. Simulations of the martian hydrologic cycle with a general circulation model: Implications for the ancient martian climate. *Icarus* **226,** 229–250 (2013).
25. Ramirez, R. M. *et al.* Warming early Mars with CO_2 and H_2. *Nature Geosci.* **7,** 59–63 (2014).
26. Catling, D. C. in *Encyclopedia of Paleoclimatology and Ancient Environments* (ed. Gornitz, V.) 66–75 (Springer, 2009).
27. Van Berk, W., Fu, Y. & Ilger, J-M. Reproducing early martian atmospheric carbon dioxide partial pressure by modeling the formation of Mg–Fe–Ca carbonate identified in the Comanche rock outcrops on Mars. *J. Geophys. Res.* **117,** E10008 (2012).

28. Som, S., Catling, D., Harnmeijer, J., Polivka, P. & Buick, R. Air density 2.7 billion years ago limited to less than twice present levels by fossil raindrop imprints. *Nature* **484,** 359–362 (2012).
29. McEwen, A. S. & Bierhaus, E. B. The importance of secondary cratering to age constraints on planetary surfaces. *Ann. Rev. Earth Planet. Sci.* **34,** 535–567 (2006).
30. Werner, S. C., Ivanov, B. A. & Neukum, G. Theoretical analysis of secondary cratering on Mars and an image-based study on the Cerberus Plains. *Icarus* **200,** 406–417 (2009).
31. Robbins, S. J., Di Achille, G. & Hynek, B. M. The volcanic history of Mars: High-resolution crater-based studies of the calderas of 20 volcanoes. *Icarus* **211,** 1179–1203 (2011).
32. Cassata, W. *et al.* Trapped Ar isotopes in meteorite ALH 84001 indicate Mars did not have a thick ancient atmosphere. *Earth Planet. Sci. Lett.* **221,** 461–465 (2012).

Acknowledgements

We thank I. Daubar, J. Dufek, B. Ehlmann, W. Fischer, V. Ganti, I. Halevy, J. Kasting, K. Lewis, M. Manga, R. Ramirez, M. Rice, A. Soto and R. Wordsworth for preprints and discussions. We thank the HiRISE team and the CTX team. This work was financially supported by an O.K. Earl Fellowship (to E.S.K.) and by the US taxpayer through NASA grants NNX11AF51G (to O.A.) and NNX11AQ64G (to J-P.W.).

Author contributions

E.S.K. designed research, picked craters, carried out the data–model comparison and drafted the main text. J-P.W. wrote the forward model of impactor–atmosphere interactions. A.L. built the digital terrain models and wrote the corresponding Supplementary text. O.A. supervised research. All authors contributed to the interpretation of the results and to the revisions.

Additional information

Supplementary information is available in the online version of the paper. Reprints and permissions information is available online at www.nature.com/reprints. Correspondence and requests for materials should be addressed to E.S.K.

Competing financial interests

The authors declare no competing financial interests.